

# Application News

No. SCA-116-003

Spectroscopy – Inductively Coupled Plasma Mass Spectrometry

## Elemental bioimaging of Al<sub>2</sub>O<sub>3</sub>/ZrO<sub>2</sub>/TiO<sub>2</sub> nanoparticles in lung tissue

Jennifer-Christin Müller<sup>1</sup>, Michael Sperling<sup>1</sup>, Uwe Karst<sup>1</sup>

<sup>1</sup> Institute of Inorganic and Analytical Chemistry, University of Münster, Germany

### ■ Introduction

Nanotechnology is one of the key developments of the 21<sup>st</sup> century. Nanoparticles are used in a wide variety of industrial, military and medical applications. Titanium dioxide (TiO<sub>2</sub>) nanoparticles are one of the most frequently used nanomaterials, for example in sunscreens as UV blocker or as antibacterial textile coating. Aluminum oxide (Al<sub>2</sub>O<sub>3</sub>) nanoparticles are used as abrasion-resistant coating in the automobile industry. In addition to that, grinding dusts can contain Al<sub>2</sub>O<sub>3</sub> as well as zirconium dioxide (ZrO<sub>2</sub>) nanoparticles.

Because of the small diameter, the nanoparticles can enter the body through the lungs and are able to cause inflammation or cell defects in the lung tissue. To be able to assess the long-term toxicity of nanoparticles, the distribution in affected organs plays an important role. Elemental bioimaging by means of laser ablation-inductively coupled plasma-mass spectrometry (LA-ICP-MS) is a useful tool to analyze various elements in tissue sections. Here, the distribution and concentration of mixed oxide nanoparticles in rat lung tissue was analyzed.

### ■ Material and methods

#### Animal study

The animal study and organ preparation were performed by IBE R&D gGmbH. The used nanoparticles were composed of aluminum(III) oxide (77% w/w), zirconium(IV) dioxide (12% w/w) and titanium(IV) dioxide (11% w/w) with a d50 value of approx. 35 nm. The nanoparticles were

intratracheally instilled into the left lung in 0.9% sodium chloride solution with an addition of 0.025 mg/ml lecithin. The instilled nanoparticle concentration was 4.8 mg per lung. The rats were euthanized three days after the instillation. The lungs were filled with an embedding media to avoid collapsing of the organ and snap-frozen afterwards. Tissue sections with a thickness of 10 µm were prepared using a cryotome and subsequently mounted on a microscope slide.

#### Standard preparation

To quantify the nanoparticle concentration in the lung, an external calibration with matrix-matched standards was performed. Gelatin (10% w/w) was spiked the nanoparticle dispersion to obtain standards with different aluminum, titanium and zirconium concentrations. Thin sections with the same thickness as the tissue sample were prepared and analyzed with the same measurement parameters.

#### Analytical conditions

For elemental bioimaging of tissue samples, LA-ICP-MS is the analytical method of choice. Here, the ICPMS-2030 quadrupole mass spectrometer was coupled to a laser ablation system LSX-213 G2<sup>+</sup> (Teledyne CETAC). The system was equipped with a Nd-YAG laser operating at a wavelength of 213 nm. The laser ablation was connected to the ICP-MS via Tygon<sup>®</sup> tubing attached to the expansion pipe. The ablation cell was flushed with helium.

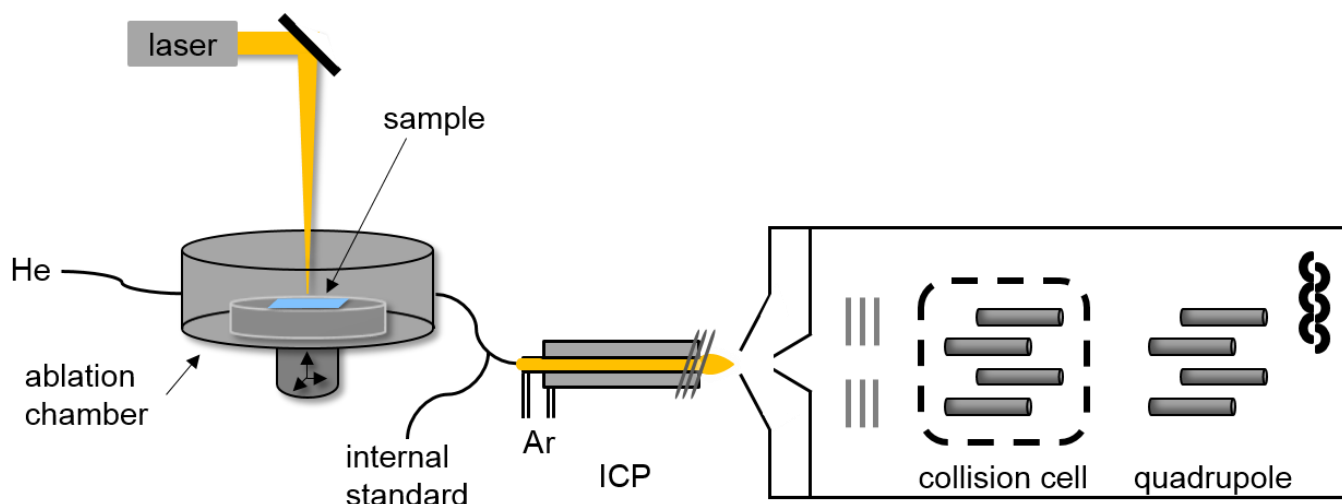


Figure 1: Schematic drawing of the LA-ICP-MS setup with internal standard introduction.

Table 1: LA and ICP-MS conditions.

Laser ablation	LSX-213 G2 <sup>+</sup>
Spot size	50 $\mu\text{m}$
Scan speed	100 $\mu\text{m}$
Shot frequency	20 Hz
Cell gas flow	0.8 l/min
ICP-MS	ICPMS-2030
Plasma power	1.2 kW
Sampling depth	5.0 mm
Plasma gas	8.0 l/min
Auxiliary gas	1.10 l/min
Carrier gas	0.45 l/min
Cell gas	6.0 ml/min
Cell voltage	-21 V

To monitor the plasma stability, an internal standard containing 1 ng/g rhodium in 2% HNO<sub>3</sub> was introduced via the nebulizer. The used setup is schematically shown in Figure 1. The ICP-MS was equipped with copper sampler and skimmer. To avoid polyatomic interferences, it was operated in the collision mode with helium as collision gas. The isotopes <sup>27</sup>Al, <sup>47</sup>Ti, <sup>49</sup>Ti, and <sup>91</sup>Zr were measured with an integration time of 0.1 s each, the isotopes <sup>31</sup>P and <sup>103</sup>Rh were measured for 0.05 s each.

## ■ Results

The rhodium signal, which was used as internal standard, has a low standard deviation of approx. 4.4%, indicating a good plasma stability during the ablation process. Limits of detection and quantification for analysis with a laser spot size of 50  $\mu\text{m}$  (Table 2) were sufficient for the expected nanoparticle concentration in the lung tissue.

In Figure 2, the bright field microscopic image as well as the LA-ICP-MS images for the <sup>31</sup>P, <sup>27</sup>Al, <sup>47</sup>Ti and <sup>91</sup>Zr distribution are shown. The endogenous element phosphorous can be used to illustrate the tissue structure with the larger air-filled bronchial tubes and smaller bronchioles and alveoli, because of its occurrence for example in phospholipids.

Table 2: Limits of detection and quantification.

Isotope	LOD [ $\mu\text{g/g}$ ]	LOQ [ $\mu\text{g/g}$ ]
<sup>27</sup> Al	65.1	217.0
<sup>47</sup> Ti	1.4	4.8
<sup>49</sup> Ti	1.6	5.2
<sup>91</sup> Zr	1.4	4.6

The aluminum, titanium and zirconium distributions are very similar, leading to the conclusion that the observed signals of those elements belong in fact to the instilled nanoparticles. With the matrix matched external calibration, aluminum concentrations up to 2500  $\mu\text{g/g}$  were found. In contrast to that, titanium concentrations up to 500  $\mu\text{g/g}$ , as well as zirconium concentrations up to 750  $\mu\text{g/g}$  were found. These differences can be explained with the composition of the mixed oxide nanoparticles. The nanoparticle distribution appears to be relatively homogenous.

Some hotspots with highest concentrations can be found in lung regions with denser tissue. Those areas correlates with higher intensities in the  $^{31}\text{P}$  distribution. In contrast to that, the nanoparticle concentration in the tissue near the bronchial tubes and bronchioles is much lower, indicating a possible cleaning effect of the lung.

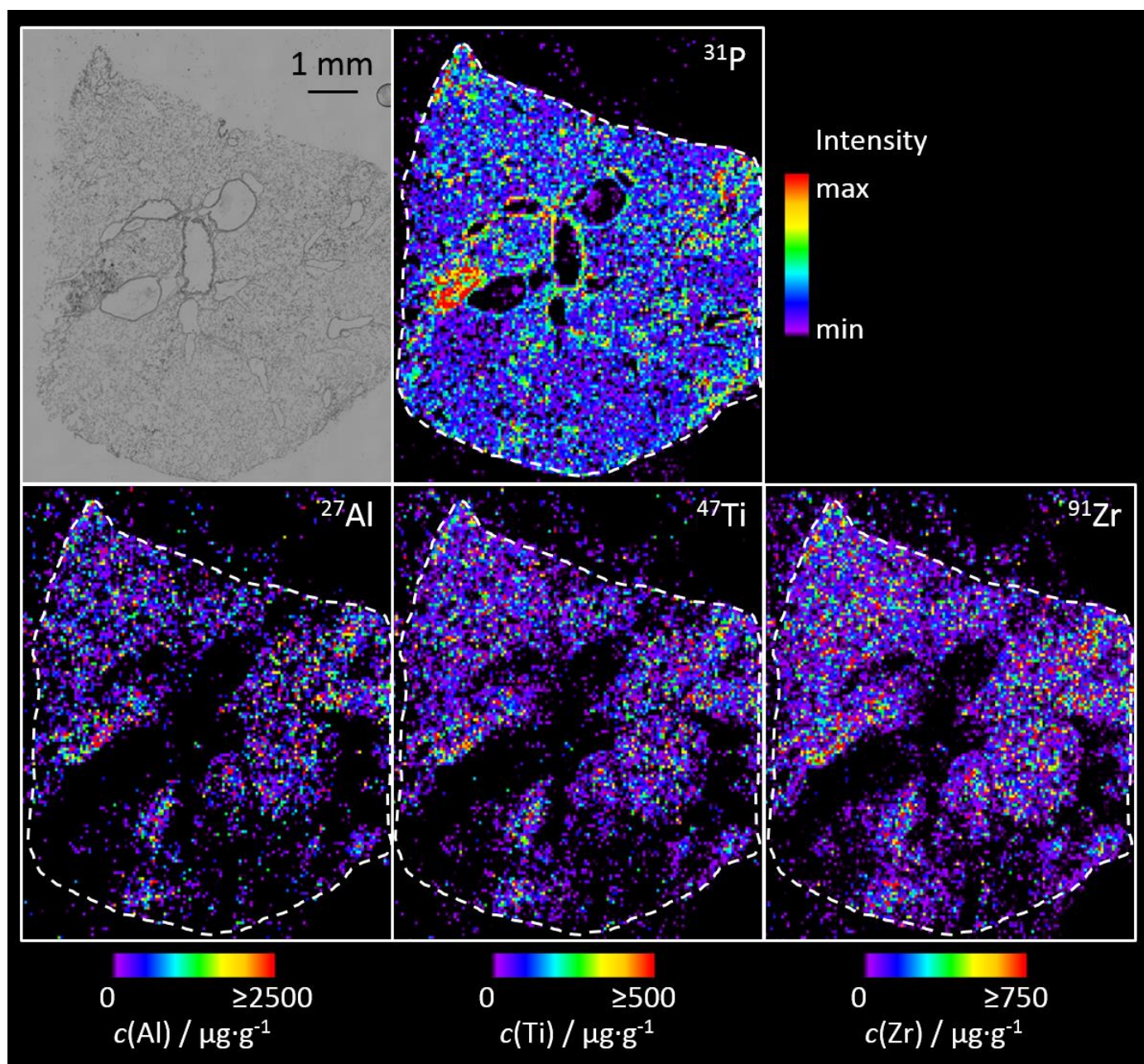


Figure 2: Bright field microscopic image (top left) as well as LA-ICP-MS images of the  $^{31}\text{P}$ ,  $^{27}\text{Al}$ ,  $^{47}\text{Ti}$ , and  $^{91}\text{Zr}$  distribution in lung tissue three days after instillation of nanoparticles. The white dotted line indicates the borders of the tissue.

## ■ Conclusion

The nanoparticle distribution in rat lung tissue was successfully visualized by means of LA-ICP-MS. The measured phosphorous distribution can be used to visualize the lung tissue. The co-localization of the three elements aluminum, titanium and zirconium, leads to the conclusion, that the observed signals can be unambiguous assigned to the instilled nanoparticles. In addition to that, the particle concentration could be determined using matrix-matched gelatin standards.

## ■ Acknowledgment

The authors thank Antje Vennemann and Martin Wiemann, IBE R&D gGmbH, for performing animal studies and sample preparation, and Maximilian Mense, Björn Ratschmeier, and Janina Anabel Werra, Institute of Inorganic and Analytical Chemistry, University of Münster, for support in measurements.

Tygon is a registered trademark of Saint-Gobain Performance Plastics Corporation.



Shimadzu Europa GmbH

[www.shimadzu.eu](http://www.shimadzu.eu)

**For Research Use Only. Not for use in diagnostic procedures.**

This publication may contain references to products that are not available in your country. Please contact us to check the availability of these products in your country.

The content of this publication shall not be reproduced, altered or sold for any commercial purpose without the written approval of Shimadzu. Company names, products/service names and logos used in this publication are trademarks and trade names of Shimadzu Corporation, its subsidiaries or its affiliates, whether or not they are used with trademark symbol "TM" or "®".

Third-party trademarks and trade names may be used in this publication to refer to either the entities or their products/services, whether or not they are used with trademark symbol "TM" or "®".

Shimadzu disclaims any proprietary interest in trademarks and trade names other than its own.

The information contained herein is provided to you "as is" without warranty of any kind including without limitation warranties as to its accuracy or completeness. Shimadzu does not assume any responsibility or liability for any damage, whether direct or indirect, relating to the use of this publication. This publication is based upon the information available to Shimadzu on or before the date of publication, and subject to change without notice.